Original Article

# Exploring the Phytopharmaceutical Potential of *Passiflora incarnata* L. in Combating Biofilm Formation and Virulence of Clinical *Acinetobacter baumannii* Isolates

Kamali Srilakshmi Ravichandran, Naji Naseef Pathoor, Pitchaipillai Sankar Ganesh, Geetha Royapuram Veeraragavan

DOI: 10.34172/PS.026.43311

To appear in: Pharmaceutical Science (https://pstbzmed.com/)

Received date: 30 Sep 2025

Revised date: 23 Feb 2026

Accepted date: 23 Feb 2026

Please cite this article as: Ravichandran KS, Pathoor NN, Ganesh PS, Veeraragavan GR. Exploring the phytopharmaceutical potential of Passiflora incarnata L. in combating biofilm formation and virulence of clinical Acinetobacter baumannii isolates. Pharm Sci. 2026. doi: 10.34172/PS.026.43311

**Exploring the Phytopharmaceutical Potential of *Passiflora incarnata L.* in Combating Biofilm Formation and Virulence of Clinical *Acinetobacter baumannii* Isolates**

Kamali Srilakshmi Ravichandran[1#], Naji Naseef Pathoor[2#], Pitchaipillai Sankar Ganesh[2*], Geetha Royapuram Veeraragavan[2]

[1] Bachelor of Dental Surgery, Saveetha Dental College and Hospitals, Saveetha Institute of Medical and Technical Sciences (SIMATS), Saveetha University (Deemed to be University), Chennai-600 077, Tamil Nadu, India.

[2] Department of Microbiology, Centre for infectious Diseases, Saveetha Dental College and Hospitals, Saveetha Institute of Medical and Technical Sciences (SIMATS), Saveetha University (Deemed to be University), Chennai-600 077, Tamil Nadu, India.

[#] Equal contribution

[*]**Corresponding author:** Dr. Pitchaipillai Sankar Ganesh, Department of Microbiology, Centre for infectious Diseases, Saveetha Dental College and Hospitals, Saveetha Institute of Medical and Technical Sciences (SIMATS), Saveetha University (Deemed to be University), Chennai-600 077, Tamil Nadu, India. Email: p_sankarganesh@hotmail.com

**Running Article:** Pharmaceutical potential of *P. incarnata* against *A. baumannii*

**Abstract**

**Background:** Biofilm-associated infections caused by multidrug-resistant (MDR) *Acinetobacter baumannii* (*A. baumannii*) pose a major therapeutic challenge due to persistent colonization and limited treatment options. Natural products are increasingly investigated as antivirulence agents capable of disrupting biofilm formation and motility without imposing strong bactericidal pressure. *Passiflora incarnata* (*P. incarnata*), a flavonoid-rich medicinal plant, has shown promising antimicrobial potential. This study examined the ability of *P. incarnata* extract to modulate biofilm formation, virulence traits, and quorum sensing (QS) related targets in clinical *A. baumannii* isolates.

**Methods:** Clinical *A. baumannii* isolates (CUAB-01–CUAB-04) were confirmed by MALDI-TOF and tested for antibiotic susceptibility. Antibacterial activity of *P. incarnata* extract was

evaluated by well-diffusion and broth microdilution assays to determine MIC. Sub-MIC levels were used to assess biofilm inhibition, alginate production, growth kinetics, swarming and twitching motility, and $H_2O_2$ sensitivity. Biofilm architecture was examined on coverslips using light microscopy. Furthermore, molecular docking of orientin and vitexin with QS related targets (7ZL4, 5HM6) was carried out using AutoDock Vina to predict binding affinities and key interactions.

**Results:** *P. incarnata* extract demonstrated clear antibacterial activity with a MIC of 0.625 mg/mL, A sub-MIC of 0.312 mg/mL significantly reduced biofilm biomass without affecting planktonic growth. Sub-inhibitory treatment also led to reduced alginate production, impaired swarming and twitching motility, and heightened susceptibility to oxidative stress. Microscopy revealed disrupted, sparse biofilm architecture in treated samples. Docking analysis revealed favorable binding affinities of orientin and vitexin toward 7ZL4 and 5HM6, suggesting potential targeting of QS and biofilm regulatory proteins.

**Conclusion:** *P. incarnata* exhibits strong antibacterial, antibiofilm, and antivirulence effects against clinical MDR *A. baumannii*, particularly at sub-MIC levels by suppressing the pathogenic traits. These findings highlight its potential as a natural therapeutic candidate for managing persistent *A. baumannii* biofilm infections and warrant further *in-vivo* and mechanistic investigations.

**Keywords:** *Acinetobacter baumannii, Passiflora incarnata,* biofilm, virulence factors, quorum sensing, molecular docking,

## Introduction

*Acinetobacter baumannii* (*A. baumannii*) has emerged as one of the most formidable threats in clinical microbiology, largely due to its considerable capacity to acquire antibiotic resistance and persist in hospital environments through biofilm formation.[1] This opportunistic Gram-negative pathogen responsible for a significant proportion of hospital-acquired infections worldwide, including wound infections, meningitis, urinary tract infections, bacteremia, and several other conditions, particularly among ICU patients.[2] Recognizing the severe threat posed by multidrug-resistant (MDR) and extensively drug-resistant (XDR) strains, the World Health Organization (WHO) classified *A. baumannii* as a top-priority 'critical' pathogen due to its high morbidity and mortality rates.[3]

A key factor in *A. baumannii* pathogenic efficiency is its strong ability to form protective biofilms. These biofilms, comprising bacterial communities within an extracellular polymeric substance (EPS) matrix, shield the bacteria from host immune responses, harsh environments, and antibiotic therapies.[4,5] These sessile communities readily develop on various medical devices, including ventilators, prosthetic joints, and catheters. Their ability to persist on such equipment promotes chronic infections that are difficult to manage in hospital settings.[4,5]

Biofilm formation in *A. baumannii* is driven by a network of coordinated virulence determinants, including surface structures, extracellular polymers, and regulatory circuits.[6] Pili and other adhesins initiate attachment and facilitate surface-associated motility, enabling the bacterium to effectively colonize both biotic and abiotic surfaces.[7] Outer membrane proteins such as OmpA strengthen adhesion, promote microcolony formation, and contribute to host cell damage.[6] Polysaccharides like PNAG provide structural stability and protect the embedded cells from immune clearance and antimicrobial stress.[6] Quorum sensing (QS) tightly regulates these processes, synchronizing adhesion, motility, EPS production, and dispersal to optimize survival under host and environmental pressures.[7,8] Together, these integrated factors drive robust biofilm development while enhancing overall virulence and persistence.

The rapid development of antibiotic resistance in *A. baumannii* underscores the urgent need for alternative therapeutic strategies.[9] However, despite extensive insights into its virulence and biofilm-regulatory mechanisms, only a limited number of studies have explored natural compounds capable of targeting QS-mediated motility and biofilm formation in clinical isolates. This gap highlights the growing importance of identifying antivirulence agents that do not exert conventional bactericidal pressure. In this context, natural products particularly herbal extracts are gaining significant attention for their antibiofilm and antivirulence potential.[10] *Passiflora incarnata* L. (*P. incarnata*) is a traditionally valued medicinal plant rich in flavonoids, alkaloids, phenolics, glycosides, and acetylenic derivatives. Its phytochemicals exhibit antibacterial, antibiofilm, antioxidant, and anti-inflammatory activities.[10] *Passiflora* have also been noted for their potential to influence bacterial surface interactions, which may play a role in modulating early biofilm development.[10] Moreover, copper oxide nanoparticles synthesized from Passiflora leaf extracts have demonstrated enhanced antibacterial and antibiofilm activity, highlighting its potential for future therapeutic applications.[11]

Beyond its antimicrobial properties, *P. incarnata* has long been used in traditional and modern medicine to treat anxiety, insomnia, and stress-related disorders.[12] Although widely explored for its pharmacological benefits, little is known about its anti-QS activity or its ability to inhibit *A. baumannii* motility and biofilm formation. In this study, we present the first comprehensive evaluation of *P. incarnata* herbal extract against key QS-regulated virulence traits in clinical *A. baumannii* isolates, demonstrating its capacity to disrupt motility, suppress biofilm development, and attenuate associated pathogenic factors. To our knowledge, this is the first investigation to delineate both the anti-QS and antibiofilm effects of *P. incarnata* against *A. baumannii***,** underscoring its potential as a promising natural therapeutic candidate for managing persistent, biofilm-associated infections.

## Methodology

### *Culture Conditions of A. baumannii***.**

The clinical isolates of *Acinetobacter baumannii (A. baumannii)* isolates used in this investigation were procured from the Central University of Tamil Nadu, India, Department of

Biotechnology (CUAB-01, CUAB-02, CUAB-03, CUAB-04). Initial genus and species identification was carried out using standard microbiological protocols, as described in previous studies.[13] By the use of the VITEK MS PRIME MALDI-TOF Mass Spectrometry System (BioMérieux, Paris, France), these isolates were confirmed *A. baumannii* after resurrection.[14] Prior to experimental use, cultures were streaked on Luria–Bertani (LB) agar plates and incubated at 37 °C for 18–24 h to obtain single colonies. Fresh overnight cultures were then prepared in LB broth at 37 °C with shaking at 180 rpm.

***P. incarnata herbal extract.***

The study utilized herbal powder extract of *Passiflora incarnata* (*P. incarnata*), generously provided by Vedic Herbs, India. The powder was derived specifically from the flowers of *P. incarnata*, which are rich in key bioactive flavonoids. The botanical identity of the plant material was authenticated by independent qualified researchers prior to use. The extract supplied by the manufacturer was stored at room temperature according to recommended conditions. For experimental assays, the powder extract was dissolved in Dimethyl Sulfoxide (DMSO), a widely used solvent with high solubilizing efficiency and proven ability to preserve the stability of plant-derived bioactive constituents.

**Evaluation of antibiotic susceptibility and the antimicrobial potential of *P. incarnata* against *A. baumannii* isolates**

Antibiotic susceptibility testing was performed using various antibiotics against CUAB-01, CUAB-02, CUAB-03, CUAB-04 to determine the resistance and sensitivity profile of the bacterium as well as its overall resistance potential. Following this, the antimicrobial activity of *P. incarnata* extract was assessed using well agar diffusion technique according to standard procedures.[15] In brief, a sterile swab was used to evenly spread an overnight culture of *A. baumannii* strains onto MHA plates (HiMedia, Mumbai, India). After making well on the agar surface, 40 µL of the *P. incarnata* extract, which was taken at a concentration of 10 mg/mL in DMSO, was poured. In addition, Ciprofloxacin (10 µg/mL) was used as the positive control, whereas DMSO served as the negative control to validate antimicrobial activity and ensure experimental reliability. Following 24 h of incubation at 37 °C, antibacterial activity was evaluated by measuring the inhibition zone diameters using a

vernier caliper. Subsequent analyses focused on the most resistant isolates, CUAB-01 to CUAB-04.

***MIC Determination.***

Following accepted procedures, the MIC of *P. incarnata* extract was evaluated against isolate CUAB-01.[16] The extract was prepared in a twofold serial dilution range from 10 mg/mL to 0.019 mg/mL. A bacterial suspension (20 µL; 0.5 McFarland ≈ 1.5 × $10^8$ CFU/mL) was inoculated in LB broth with serially diluted extract and incubated at 37 °C for 24 h. Afterall, 30 µL TTC was added, and results were noted after 30 min. Tubes showing no color change at the lowest extract concentration indicated the MIC. These findings were subsequently utilized to design antibiofilm assays.

***Evaluation of Biofilm Inhibitory Activity.***

Using the CV staining method, the biofilm inhibition caused by *P. incarnata* extract was assessed.[16] In brief, overnight cultures of CUAB-01 (20 µL) were inoculated into LB broth (180 µL) in 96-well plates and treated with two-fold serial dilutions of the extract, ranging from 0.312 mg/mL to 0.0006 mg/mL. Plates were incubated at 37 °C for 48 h, washed gently, and the resulting biofilms were stained with 0.1% crystal violet (CV). After rinsing, the bound dye was solubilized with 70% ethanol, and the absorbance was measured at 520 nm to quantify biofilm biomass, while absorbance at 600 nm was recorded to assess planktonic cell growth.

using the following formula, the amount of biofilm inhibition was determined:

$$\text{Control OD } 520\text{nm} - \text{Treated OD } 520\text{nm} / \text{Control OD } 520\text{nm} \times 100$$

Additionally, the same CV staining procedure was also used in glass test tubes to evaluate the biofilm inhibition caused by *P. incarnata* extract, but without ethanol solubilization. To assess biomass and homogeneity in response to the extract treatment, biofilm growth on the tube walls was examined visually following incubation and staining.

***Alginate quantification in CUAB-01.***

Alginate levels in CUAB-01 were measured using a carbazole-based quantification method. Briefly, a boric acid-sulfuric acid mixture (4:1) was added to the cell suspension, followed by

carbazole reagent, and incubated at 55 °C for 30 min. Absorbance was measured at 530 nm to compare alginate levels in CUAB-01 with and without *P. incarnata* treatment.

***CUAB-01 Growth Kinetics.***

Both with and without *P. incarnata* extract, CUAB-01 growth was observed at a dosage of 0.312 mg/mL. As the culture media was incubated for 24 h at 37°C, the cell density was recorded hourly at OD600.

***Evaluation of bacterial translocation on surfaces and pilus-driven twitching motility.*** Swarming motility of CUAB-01 was assessed using a previously described protocol.[17] MHA (0.5% agar) plates with or without *P. incarnata* extract (0.312 mg/mL) were spot-inoculated with 5 µL overnight culture and incubated at 37 °C for 72 h. Swarming zone diameters were measured to compare treated and control groups. Additionally, for the twitching motility assay, a sterile toothpick was used to stab-inoculate overnight bacterial cultures (treated and control) at the center of a 1% LB agar plate, ensuring penetration to the bottom of the agar. The plates were then incubated for 72 h. After incubation, the agar surface was gently washed with PBS, and the twitching zone was stained using 0.4% CV solution.

***Reactive Oxygen Species (ROS) Sensitivity Assay.***

The sensitivity of CUAB-01 to $H_2O_2$ was tested by disc diffusion.[18] MHA plates with or without *P. incarnata* extract (0.312 mg/mL) were inoculated, and sterile discs loaded with 8 µL $H_2O_2$ were placed at the center. To evaluate the impact of the extract on $H_2O_2$ sensitivity, plates were incubated for 18 h at 37 °C, and the widths of the inhibitory zones were determined.

***Microscopic examination of CUAB-01 biofilm.***

Microscopy was used to study biofilm formation on glass coverslips as described previously by Pathoor et al (2024).[19] Overnight CUAB-01 cultures were incubated in fresh LB medium with coverslips, untreated (control) and treated with 0.312 mg/mL *P. incarnata* extract, at 24 h under static conditions (37 °C). After incubation, coverslips were washed with sterile water, stained with 0.2% CV, rinsed again, and biofilms were observed under a contrast microscope (Olympus CX23, China).

***Insilco analysis of flavonoids constituents from P. incarnata dry extract.*** Molecular docking studies were performed flavonoid compounds identified from the *P. incarnata* dry extract. Key flavonoid compounds were isolated from the dried extract of *P. incarnata* using a previously well-described HPLC protocol reported by Guseinov MD et al (2019).[20] The HPLC analysis revealed numerous bioactive flavonoids within the extract. Among the various flavonoid compounds identified, Orientin and Vitexin emerged as the predominant constituents of PDE, accounting for relative abundances of 29.78% and 23.06%, respectively, as reported by Guseinov MD et al (2019).[20] In our study, we assessed the binding affinities of orientin and vitexin through molecular docking, highlighting their potential for subsequent biochemical and pharmacological investigations.

***Molecular docking and interaction profiling.***

Orientin ($C_{21}H_{20}O_{11}$; PubChem CID: 5281675) has a molecular weight of 448.4 g/mol and is composed of 21 carbons, 20 hydrogens, and 11 oxygens. Vitexin ($C_{21}H_{20}O_{10}$; PubChem CID: 5280441) weighs 432.4 g/mol and contains 21 carbons, 20 hydrogens, and 10 oxygens. Both flavonoids were identified through their characteristic peaks in the HPLC-UV chromatogram of the PDE flavonoid profile, as reported by the recent study of Guseinov MD et al (2019).[20] Orientin exhibited the greatest relative abundance with a peak area of 1026, corresponding to 29.78% of the total chromatographic peak area, while Vitexin was also present with a peak area of 794,4 accounting for 23.06%. Their structures were corroborated by data sourced from the PubChem database (NCBI, NIH) for orientin (CID: 5281675) and vitexin (CID: 5280441).

***Molecular docking: Structural analysis and binding interactions.***

In this study we focused on two essential proteins from *A. baumannii*: 7ZL4, representing the cryo-electron microscopy structure of the ancient chaperone-usher *Csu* pilus system, and 5HM6, which corresponds to the N-terminal region of the *BfmR* transcriptional regulator. These proteins are crucial for biofilm development and disease-causing mechanisms in *A. baumannii*. The Protein Data Bank provided the three-dimensional structures (RCSB PDB). The protein structures were visualized and prepared, which included removing extraneous elements including water molecules, extra ligands, and superfluous

protein chains. Atomic charges and polar hydrogen atoms were added with BIOVIA Discovery Studio Visualizer 2024 (v24.1.0.23298, Dassault Systèmes Biovia Corp.).

The 7ZL4 protein serves as a key mediator in cellular attachment and biofilm establishment. Its distinctive structural characteristics and flexibility allow it to bind with host cell surfaces, thus triggering infectious processes. This protein demonstrates structural adaptability during host cell interactions, allowing modification by host enzymes and supporting immune system evasion through the masking of antibody recognition sites. Likewise, the 5HM6 protein, functioning as the *BfmR* transcriptional regulator, is vital for controlling genes involved in biofilm production, environmental stress responses, and pathogenic factors in *A. baumannii*.

Computational docking analyses were conducted to examine how vitexin and orientin interact with these target proteins. The docking process utilized PyRx-Python Prescription 0.8 incorporating AutoDock Vina as the computational docking platform. Various molecular conformations were produced, and the most favorable docking configuration for each protein-compound pair was selected based on the most negative binding energy values. The final binding patterns and three-dimensional arrangements were subsequently examined and displayed using BIOVIA Discovery Studio Visualizer 2024.

**Statistical analysis**

To ensure precision and consistency, every experiment was carried out in triplicate. Data are presented as mean ± standard deviation (SD). One-way ANOVA (Tukey's post hoc test in GraphPad Prism 5.03 (GraphPad Software Inc., La Jolla, CA, USA) was used to evaluate the data. A p-value of $< 0.05$ was considered statistically significant. Comparisons with the control group are represented as $*p < 0.05$, $**p < 0.01$, and $***p < 0.001$.

**Results**

**Biochemical Profiling and Antimicrobial Testing**

*A. baumannii* strains characterized as a rod-shaped, Gram-negative bacterium through Gram staining. The isolates showed positive results for catalase and citrate utilization tests.

The clinical isolate CUAB-01 of *A. baumannii* exhibited high resistance to most tested antibiotics, including gentamicin, cefixime, ceftriaxone, imipenem, meropenem, and tetracycline, according to antibiotic susceptibility testing. In addition, CUAB-02 was sensitive to piperacillin-tazobactam, gentamicin, imipenem, and tetracycline, while CUAB-03 and CUAB-04 showed sensitivity to gentamicin, imipenem, ceftriaxone, piperacillin-tazobactam, and tetracycline. These results highlight the significant MDR profile of CUAB-01. Moreover, the antimicrobial efficacy of *P. incarnata* extract against *A. baumannii* isolates was demonstrated, with the extract producing an inhibition zone of 12 mm for CUAB-01, 14 mm for CUAB-02 and CUAB-03, and 15 mm for CUAB-04. Subsequent experiments were conducted using CUAB-01.

***Inhibitory effect of P. incarnata on CUAB-01***

Using doses ranging from 10 mg/mL to 0.019 mg/mL, the antibacterial efficacy of *P. incarnata* extract was assessed using a two-fold serial dilution technique. With a MIC of 0.625 mg/mL, the extract inhibited the growth of CUAB-01.

***P. incarnata inhibits the production of biofilms in CUAB-01***

The impact of *P. incarnata* extract on the biofilm-forming ability of CUAB-01 was assessed using a static microtiter plate assay with 0.1% CV staining. Treatment with the extract markedly reduced biofilm formation compared to the untreated control. Spectrophotometric measurements showed biofilm inhibition of 52.11% at 0.312 mg/mL and 25.22% at 0.156 mg/mL. Figure 1A shows percentage biofilm inhibition measured at 520 nm, demonstrating the dose-dependent antibiofilm activity of *P. incarnata* against CUAB-01, while the absorbance at 600 nm reflects the corresponding bacterial growth. Figure 1B illustrates visual tube assay results, showing that *P. incarnata* markedly reduced ring biofilm formation at both concentrations, while the untreated control displayed a strong and well-defined ring biofilm.

***Alginate quantification in CUAB-01***

A component of the extracellular polymeric matrix, alginate is vital for protecting bacterial cells and maintaining biofilm stability. There was a noticeable drop in alginate synthesis when CUAB-01 was exposed to sub-inhibitory doses of *P. incarnata*. The most pronounced reduction was observed at 0.312 mg/mL, which resulted in a 40.28% decrease in alginate levels, followed by 0.156 mg/mL, which produced a 27.96% reduction, as shown in the Figure 2**,** where alginate quantification was measured spectrophotometrically at 530 nm.

***Analysis of Growth Profile***

Using *P. incarnata* extract, the growth behaviour of CUAB-01 was investigated both with and without treatment. The extract at 0.312 mg/mL did not significantly affect bacterial growth, as the treated cultures showed absorbance values at 600 nm comparable to the untreated control. Figure 3 presents the growth curve data, with absorbance at 600 nm plotted on the y-axis and incubation time on the x-axis, confirming that *P. incarnata* did not inhibit CUAB-01 growth at this concentration.

***Inhibition of Surface Migration and Twitching Motility in CUAB-01 by P. Incarnata***

Swarming motility assays were conducted to evaluate the influence of *P. incarnata* extract on the movement of CUAB-01. This bacterium typically utilizes flagella and pili to facilitate motility, surface adherence, and environmental adaptation. Our findings revealed that treatment with *P. incarnata* markedly impaired swarming activity. At a concentration of 0.312 mg/mL, the extract caused a pronounced reduction in motility compared to the vigorous swarming displayed by the untreated control, as shown in the Figure 4A. Additionally, at the same concentration of *P. incarnata*, there was a substantial decrease in twitching motility as compared to the control group, as illustrated in Figure 4B.

***Treatment with P. incarnata increased the susceptibility of CUAB-01 towards $H_2O_2$***

Neutrophils and macrophages, key innate phagocytes, generate reactive oxygen species (ROS) to mediate intracellular bacterial clearance.[21] To evaluate whether *P.*

*incarnata* influences the susceptibility of CUAB-01 to ROS, a $H_2O_2$ sensitivity assay was performed. In the disc diffusion assay, the control plate exhibited a zone of 16 mm, which increased to 32 mm following treatment with 0.312 mg/mL *P. incarnata* extract, as shown in the Figure 5.

**Analysis of *In-situ imaging.***

Biofilm clustering was shown to be reduced in *P. incarnata*-treated CUAB-01, as determined by *in-situ* imaging. We used inverted phase-contrast microscopy to evaluate *P. incarnata* impact on biofilm formation. Direct light microscopic examination revealed a marked decline in biofilm clusters in the treated samples (Figure 6), whereas the control displayed dense aggregates and extensive biofilm formation accompanied by diffuse extracellular polymeric substances.

***In silico Analysis of Orientin and Vitexin with A. baumannii Regulators 7ZL4 and 5HM6.***

Docking simulations were conducted to assess the binding interactions of Orientin and Vitexin with *A. baumannii* regulators 5HM6 and 7ZL4 (Figure S1:S2). Vitexin bound to 5HM6 and 7ZL4 with affinities of –6.2 kcal/mol and –6.5 kcal/mol, respectively, whereas Orientin showed higher binding affinities of –6.6 kcal/mol and –8.7 kcal/mol with the same proteins (Table 1A:1B).

For the 5HM6 regulator, Vitexin established a conventional hydrogen bond and a π-donor hydrogen bond with VAL A:109, along with additional hydrophobic interactions through π-alkyl (PRO A:111) and π–sigma (LEU A:22) contacts. In the case of 7ZL4, Vitexin formed three conventional hydrogen bonds with GLY B:36 and PHE B:36, as well as a carbon hydrogen bond with ASN B:34. Furthermore, it engaged in extensive hydrophobic interactions, comprising four π-alkyl and five alkyl contacts, involving residues TRP B:42, ILE B:132, LEU B:85, VAL B:95, TYR B:145, and LYS B:140.

By comparison, Orientin demonstrated a greater number of stabilizing interactions, consistent with its stronger binding affinity. With 5HM6, Orientin formed five hydrogen bonds involving ASP A:16, LEU A:19, THR A:23, and VAL A:109, along with two π-alkyl interactions with PRO A:108. For the 7ZL4 regulator, Orientin generated two conventional hydrogen bonds (GLY B:36, LYS B:140), a carbon hydrogen bond (ASP B:144), one π-alkyl

interaction with LYS B:37, a π–π stacked interaction with TYR B:145, and a π-anion interaction with ASP B:144. Overall, the Orientin-7ZL4 complex comprised two conventional hydrogen bonds, one carbon hydrogen bond, and three additional non-covalent interactions (π-alkyl, π–π stacked, and π-anion).

These findings suggest that both Orientin and Vitexin exhibit notable interactions (Table S1A:S2B). However, additional validation through advanced assays, including *in-vivo* studies, is essential to confirm the antibiofilm potential of these compounds.

**Discussions**

*A. baumannii* infections are difficult to treat owing to both its potent biofilm formation and broad-spectrum antibiotic resistance.[22] *A. baumannii* employs complex biofilm formation mechanisms involving pili, outer membrane proteins, and QS systems that regulate virulence factor production and biofilm maturation, thereby enhancing its survival in hospital environments.[23,24] Disrupting biofilm formation and QS pathways has emerged as a promising therapeutic strategy against *A. baumannii*. Several natural compounds, particularly flavonoid-rich extracts, have been explored for their potent antibiofilm activities.[25] Likewise, phenolic compounds derived from medicinal plants have demonstrated significant ability to suppress biofilm synthesis and downregulate virulence factor expression, further highlighting the potential of plant-based therapeutics in combating this pathogen.[26]

In our study we explored *P. incarnata* herbal extract as an antibiofilm and antivirulence agent against MDR *A. baumannii* (CUAB-01). Similarly, Ramaiya et al (2014) reported that extracts from *Clematis grata*, *Clematis viticella*, and *Berginia ciliata* achieved more than 50% inhibition of biofilm formation in Gram-negative bacteria.[26] Additionally, the QS capacity of *A. baumannii* is suppressed by siphonocholin, a steroid produced from marine creatures.[27] In preliminary analysis, the antimicrobial assay showed inhibition zones ranging from 12 to 15 mm across isolates CUAB-01 to CUAB-04. Among these, CUAB-01 exhibited the smallest inhibition zone (12 mm), indicating higher resistance and was therefore selected for further investigation. At an endpoint concentration of 0.625 mg/mL, *P. incarnata* herbal extract effectively suppressed the growth of CUAB-01, confirming its notable antimicrobial potential. The findings of our study corroborate those of Hemeg et al (2020),[28] in which

herbal extracts such as *Psidium guajava*, *Salvia officinalis*, *Ziziphus spina-christi*, *Morus alba*, and *Olea europaea* demonstrated significant antimicrobial activity. Altogether, our observations highlight *P. incarnata* as a promising natural candidate with potent activity even against highly resistant strains.

Furthermore, we examined whether *P. incarnata* could inhibit CUAB-01 QS-dependent biofilm development at sub-MIC concentrations. The biofilm assay revealed that at 0.625 mg/mL, *P. incarnata* significantly reduced the formation of biofilm clusters without affecting the proliferation of planktonic cells. These observations align with earlier findings, where ethyl acetate extracts of *Passiflora edulis* significantly inhibited biofilm formation in *Chromobacterium violaceum* at concentrations between 0.5 and 2 mg/mL.[17] Notably, our study demonstrates that effective antibiofilm activity can be achieved at comparatively lower concentrations. Previous research has consistently shown that plant-derived compounds possess strong antibiofilm properties, further underscoring their potential as effective agents for disrupting bacterial biofilms.[29,30]

Moreover, motility contributes significantly to bacterial pathogenicity by facilitating microcolony development and sustaining biofilm structural organization. Flagella, pili, and fimbriae in *A. baumannii* work together to enhance movement and promote biofilm formation. Specifically, pili facilitate twitching motility, flagella are associated with swarming behaviour, and fimbriae further support bacterial mobility, enabling colonization at interfaces such as air–liquid boundaries. These surface structures are instrumental for initial attachment to host surfaces, contributing significantly to biofilm establishment and the early stages of infection.[31] We evaluated the effects of *P. incarnata* herbal extract on CUAB-01 motility, and our outcomes implied that *P. incarnata* herbal extract have a major impact on swarming and twitching motility. Supporting this observation, a study on the closely related species *Passiflora edulis* demonstrated that ethyl acetate extracts significantly inhibited swarming motility in *C. violaceum* at concentrations of 0.5-2 mg/mL, indicating a clear dose-dependent suppression. Our findings with *P. incarnata* further support this trend, showing comparable inhibitory effects even at lower concentrations.[17] In addition, studies involving a variety of plant sources, including *Mangifera indica* and *Carex dimorpholepis*, has shown a strong inhibition of swarming motility in pathogens such as *Pseudomonas aeruginosa* and

*Escherichia coli* confirming the efficiency of secondary metabolites derived from plants in limiting bacterial surface migration.[32,33] Furthermore, *A. baumannii* defends itself against metabolic and host-derived ROS by producing antioxidant enzymes such as catalase and superoxide dismutase. These enzymes are linked to QS-mediated biofilm formation in *A. baumannii.*[34] Therefore, our evaluation of $H_2O_2$ sensitivity in CUAB-01 revealed that cells treated with *P. incarnata* herbal extract were markedly more susceptible to oxidative stress than the untreated controls. This observation is in line with the findings of Selvaraj et al (2020),[18] who reported increased $H_2O_2$ sensitivity in *A. baumannii* strains following myrtenol treatment. Notably, our results demonstrate an even more pronounced enhancement in oxidative susceptibility, underscoring the strong antivirulence potential of *P. incarnata*. Furthermore, *In-situ* microscopy was further used to assess bacterial surface features and biofilm architecture, revealing that treated CUAB-01 samples reduces the development of biofilm clusters, unlike the untreated controls.

Moreover, key flavonoid compounds were identified from the dried extract of *P. incarnata* using HPLC analysis as described by Guseinov et al. (2019)[20], with Orientin and Vitexin as the major constituents. In our study, these compounds were subjected to molecular docking with *A. baumannii* target proteins. The docking analysis revealed detailed interactions of Vitexin and Orientin with the regulatory proteins 5HM6 and 7ZL4, providing insights into their potential mechanisms of action. Vitexin displayed binding affinities of –6.2 kcal/mol with 5HM6 and –6.5 kcal/mol with 7ZL4. For 5HM6, it formed key interactions including a conventional hydrogen bond and a π-donor hydrogen bond with VAL A:109 and THR A:23 along with hydrophobic π-alkyl and π–sigma interactions with PRO A:111 and LEU A:22, respectively. These interactions suggest that Vitexin possesses notable stability and binding affinity toward the 5HM6 regulator.

In comparison, Orientin demonstrated stronger binding affinities of –6.6 kcal/mol with 5HM6 and a notably higher –8.7 kcal/mol with 7ZL4, reflecting a superior interaction profile. Orientin formed multiple stabilizing contacts with 5HM6, including five hydrogen bonds with residues ASP A:16, LEU A:19, THR A:23, and VAL A:109, along with π-alkyl interactions involving PRO A:108. This richer interaction network denotes higher binding specificity and stability.

Regarding the 7ZL4 regulator, Vitexin engaged in hydrogen bonding with GLY B:36 and PHE B:36 and a carbon-hydrogen bond with ASN B:34, along with extensive hydrophobic contacts involving residues like TRP B:42, LEU B:85, VAL B:94, ILE B:132, TYR B:145, and LYS B:140. Orientin surpassed this by forming six stabilizing interactions, including two conventional hydrogen bonds (GLY B:36, LYS B:140), a carbon-hydrogen bond (ASP B:144), a π-alkyl interaction with LYS B:37, a π-π stacked interaction with TYR B:145, and a π-anion interaction with ASP B:144. This diverse set of interactions underpins Orientin's higher binding affinity and suggests its potential as a more effective ligand for the 7ZL4 regulator.

Overall, Orientin's greater number of hydrogen bonds and varied interaction types underpin its superior binding affinity observed in docking studies. These molecular interactions likely contribute to better inhibitory potential, consistent with findings in other studies where Orientin is noted for enhanced bioactivity and antibacterial properties compared to Vitexin. This docking analysis supports the hypothesis that Orientin may be a more potent candidate for targeting these bacterial regulators, potentially leading to improved antimicrobial efficacy. Inhibiting the activity of 5HM6 and 7ZL4 key regulators associated with QS signal transduction could disrupt downstream AHL-mediated communication pathways in *A. baumannii*, thereby attenuating the expression of QS-controlled virulence factors and impairing coordinated biofilm development.

Additionally, these findings align with previous research highlighting the promising therapeutic potential of flavonoids like Orientin and Vitexin through their specific and stable interactions with bacterial proteins, reinforcing their roles in antimicrobial, and antibiofilm drug design and development.[35–37] Altogether, these results indicate that both Orientin and Vitexin possess significant interaction potential with *A. baumannii* QS regulators, with Orientin displaying comparatively stronger binding. This suggests that Orientin may serve as a more potent inhibitor of biofilm formation. Even though, further confirmation through *in-vitro* and *in-vivo* studies is essential to validate their therapeutic potential as QS and biofilm inhibitors.

Furthermore, this study has certain limitations, as the findings are based on preliminary antibiofilm and antivirulence experiments. Incorporating a reference strain and a broader set of clinical isolates would strengthen the evaluation of the extract antibiofilm and antivirulence potential. Future studies should also employ transcriptomic or proteomic

profiling to identify specific QS or oxidative stress-related genes affected by *P. incarnata*. Although the *in-vitro* results are promising, *in-vivo* validation using animal infection models or clinical trials is essential to confirm the therapeutic potential and safety of *P. incarnata* for clinical use.

**Conclusions**

The findings of our study highlight the strong therapeutic potential of *P. incarnata* against *A. baumannii*, demonstrating notable antibacterial, antibiofilm, and antivirulence activities. These results suggest that *P. incarnata* could serve as a promising candidate for managing this challenging pathogen. However, the *in-vitro* nature of the present work is a key limitation, and *in-vivo* studies are needed to validate its efficacy and safety under physiological conditions. Further research involving the isolation and characterization of the active compounds, along with comprehensive *in-vivo* evaluation, will be essential to support its clinical applicability. Overall, this study provides a solid foundation for future investigations that may lead to the development of targeted and effective therapeutic strategies for *A. baumannii* infections.

**Authors' Contribution Conceptualization:**

**Conceptualization:** Kamali Srilakshmi Ravichandran, Naji Naseef Pathoor, Pitchaipillai Sankar Ganesh

**Methodology:** Kamali Srilakshmi Ravichandran, Naji Naseef Pathoor, Geetha Royapuram Veeraragavan

**Validation:** Pitchaipillai Sankar Ganesh, Geetha Royapuram Veeraragavan

**Formal Analysis:** Naji Naseef Pathoor, Kamali Srilakshmi Ravichandran

**Investigation:** Naji Naseef Pathoor, Kamali Srilakshmi Ravichandran

**Resources:** Pitchaipillai Sankar Ganesh, Geetha Royapuram Veeraragavan

**Data Curation:** Naji Naseef Pathoor, Kamali Srilakshmi Ravichandran

**Project Administration:** Pitchaipillai Sankar Ganesh

**Supervision:** Pitchaipillai Sankar Ganesh

**Writing-original Draft:** Naji Naseef Pathoor, Kamali Srilakshmi Ravichandran

**Writing-review & Editing:** Pitchaipillai Sankar Ganesh, Geetha Royapuram Veeraragavan

**Competing Interests**

The authors declare that they have no conflict of interest.

**Ethical Approval**

Not applicable.

**Funding**

This research received no specific grant from any funding agency in the public, commercial, or not-for-profit sectors.

**Supplementary Files**

Supplementary file 1 contains Table S1, Figure S1, and Figure S2.

**References**

1. Naseef Pathoor N, Viswanathan A, Wadhwa G, Ganesh PS. Understanding the biofilm development of *Acinetobacter baumannii* and novel strategies to combat infection. APMIS. 2024;132(5):317-335. doi:10.1111/apm.13399
2. Ibrahim S, Al-Saryi N, Al-Kadmy IMS, Aziz SN. Multidrug-resistant *Acinetobacter baumannii* as an emerging concern in hospitals. Mol Biol Rep. 2021;48(10):6987-6998. doi:10.1007/s11033-021-06690-6
3. World Health Organization. Global priority list of antibiotic-resistant bacteria to guide research, discovery and development of new antibiotics. WHO; 2017 Feb 27. Reference number: WHO/EMP/IAU/2017.12.
4. Castanheira M, Mendes RE, Gales AC. Global Epidemiology and Mechanisms of Resistance of *Acinetobacter baumannii-calcoaceticus* Complex. Clin Infect Dis. 2023;76(Supplement_2):S166-S178. doi:10.1093/cid/ciad109

5. Joshua AA, Girija ASS, Ganesh PS, Priyadharsini JV. Distribution of Biofilm-associated Genes among *Acinetobacter baumannii* by in-silico PCR. J Pharm Res Int. Published online December 14, 2021:140-149. doi:10.9734/jpri/2021/v33i58A34099

6. Sherif MM, Elkhatib WF, Khalaf WS, Elleboudy NS, Abdelaziz NA. Multidrug Resistant *Acinetobacter baumannii* Biofilms: Evaluation of Phenotypic-Genotypic Association and Susceptibility to Cinnamic and Gallic Acids. Front Microbiol. 2021;12. doi:10.3389/fmicb.2021.716627

7. Vijayakumar S, Rajenderan S, Laishram S, Anandan S, Balaji V, Biswas I. Biofilm Formation and Motility Depend on the Nature of the *Acinetobacter baumannii* Clinical Isolates. Front Public Health. 2016;4. doi:10.3389/fpubh.2016.00105

8. Yadav P, Shrestha S, Basyal D, et al. Characterization and Biofilm Inhibition of Multidrug-Resistant *Acinetobacter baumannii* Isolates. Int J Microbiol. 2024;2024(1). doi:10.1155/ijm/5749982

9. Girija Ass. *Acinetobacter baumannii* as an oro-dental pathogen: a red alert!! J Appl Oral Sci. 2024;32. doi:10.1590/1678-7757-2023-0382

10. Sherif MM, Elkhatib WF, Khalaf WS, Elleboudy NS, Abdelaziz NA. Multidrug Resistant *Acinetobacter baumannii* Biofilms: Evaluation of Phenotypic-Genotypic Association and Susceptibility to Cinnamic and Gallic Acids. Front Microbiol. 2021;12. doi:10.3389/fmicb.2021.716627

11. Tassew MF, Chouhan G. Biosynthesis and antibacterial activity of Passiflora incarnata mediated copper oxide nanoparticles. Int J Health Sci (Qassim). Published online June 23, 2022:6059-6075. doi:10.53730/ijhs.v6nS4.9529

12. Michael Hsr, Mohammed Nb, Ponnusamy S, Edward Gnanaraj W. A Folk Medicine: *Passiflora incarnata* L. Phytochemical Profile with Antioxidant Potency. Turk J Pharm Sci. 2022;19(3):287-292. doi:10.4274/tjps.galenos.2021.88886

13. Baltimore : Williams & Wilkins. Bacteria -- Classification, Bacteriology -- Terminology. In library; internet archive books. 1993.

14. Bobenchik AM, Deak E, Hindler JA, Charlton CL, Humphries RM. Performance of Vitek 2 for Antimicrobial Susceptibility Testing of *Acinetobacter baumannii*, *Pseudomonas aeruginosa, and Stenotrophomonas maltophilia* with VITEK 2 (2009 FDA) and CLSI M100S 26th Edition Breakpoints. J Clin Microbiol. 2017;55(2):450-456. doi:10.1128/JCM.01859-16

15. Balouiri M, Sadiki M, Ibnsouda SK. Methods for *in-vitro* evaluating antimicrobial activity: A review. J Pharm Anal. 2016;6(2):71-79. doi:10.1016/j.jpha.2015.11.005

16. Varughese RMR, Pathoor NN, Ranganathan P, Ganesh PS. Efficacy of *Rhamnus frangula* extract against *Acinetobacter baumannii* biofilms: Histopathological evidence from *ex vivo* goat models. World Acad Sci J. 2025;7(3):36. doi:10.3892/wasj.2025.324.

17. Venkatramanan M, Sankar Ganesh P, Senthil R, et al. Inhibition of Quorum Sensing and Biofilm Formation in *Chromobacterium violaceum* by Fruit Extracts of *Passiflora edulis*. ACS Omega. 2020;5(40):25605-25616. doi:10.1021/acsomega.0c02483

18. Selvaraj A, Valliammai A, Sivasankar C, Suba M, Sakthivel G, Pandian SK. Antibiofilm and antivirulence efficacy of myrtenol enhances the antibiotic susceptibility of *Acinetobacter baumannii*. Sci Rep. 2020;10(1):21975. doi:10.1038/s41598-020-79128-x

19. Pathoor NN, Ganesh PS, Anshad AR, et al. 3-Hydroxybenzoic acid inhibits the virulence attributes and disrupts biofilm production in clinical isolates of *Acinetobacter baumannii*. Eur J Clin Microbiol Infect Dis. Published online December 30, 2024. doi:10.1007/s10096-024-05009-0

20. Guseinov MD G, Bobkova NV B, Svistunov AA S, et al. Flavonoids in *Passiflora incarnata* L. Dry Extract of Russian Origin. Pharmacognosy Journal. 2019;11(5):1143-1147. doi:10.5530/pj.2019.11.178

21. Silva MT, Correia-Neves M. Neutrophils and Macrophages: The Main Partners of Phagocyte Cell Systems. Front Immunol. 2012;3. doi:10.3389/fimmu.2012.00174

22. K S. Molecular Detection of epsA-Mediated and Extracellular Polysaccharide-Mediated Biofilm Formation Among Multidrug Resistant Strains of *Acinetobacter baumannii.* Biosci Biotechnol Res Commun. 2021;14(4):1660-1665. doi:10.21786/bbrc/14.4.43

23. Vijayashree Priyadharsini J, Smiline Girija AS, Paramasivam A. An insight into the emergence of *Acinetobacter baumannii* as an oro-dental pathogen and its drug resistance gene profile – An in-silico approach. Heliyon. 2018;4(12):e01051. doi:10.1016/j.heliyon.2018.e01051

24. Longo F, Vuotto C, Donelli G. Biofilm formation in *Acinetobacter baumannii*. *New Microbiol*. 2014;37(2):119-127.

25. Liu Y, Zhu J, Liu Z, Zhi Y, Mei C, Wang H. Flavonoids as Promising Natural Compounds for Combating Bacterial Infections. Int J Mol Sci. 2025;26(6):2455. doi:10.3390/ijms26062455

26. Ramaiya SD, Bujang JS, Zakaria MH. Assessment of Total Phenolic, Antioxidant, and Antibacterial Activities of *Passiflora* Species. Sci World J. 2014;2014:1-10. doi:10.1155/2014/167309

27. Jiao Y, Tay FR, Niu L na, Chen J hua. Advancing antimicrobial strategies for managing oral biofilm infections. Int J Oral Sci. 2019;11(3):28. doi:10.1038/s41368-019-0062-1

28. Hemeg HA, Moussa IM, Ibrahim S, et al. Antimicrobial effect of different herbal plant extracts against different microbial population. Saudi J Biol Sci. 2020;27(12):3221-3227. doi:10.1016/j.sjbs.2020.08.015

29. Silva E, Teixeira JA, Pereira MO, Rocha CMR, Sousa AM. Evolving biofilm inhibition and eradication in clinical settings through plant-based antibiofilm agents. Phytomedicine. 2023;119:154973. doi:10.1016/j.phymed.2023.154973

30. Bartels N, Argyropoulou A, Al-Ahmad A, et al. Antibiofilm potential of plant extracts: inhibiting oral microorganisms and *Streptococcus mutans*. Front Dent Med. 2025;6. doi:10.3389/fdmed.2025.1535753

31. Nait Chabane Y, Mlouka M Ben, Alexandre S, et al. Virstatin inhibits biofilm formation and motility of *Acinetobacter baumannii.* BMC Microbiol. 2014;14(1):62. doi:10.1186/1471-2180-14-62

32. Bessalah S, Khorchani T, Hammadi M, Faraz A, Mustafa A. Inhibitory potential of natural plant extracts against Escherichia coli strain isolated from diarrheic camel calve. Open Vet J. 2023;13(9):1082. doi:10.5455/OVJ.2023.v13.i9.3

33. Rütschlin S, Böttcher T. Inhibitors of Bacterial Swarming Behavior. Chem Eur J. 2020;26(5):964-979. doi:10.1002/chem.201901961

34. Bhargava N, Sharma P, Capalash N. Pyocyanin Stimulates Quorum Sensing-Mediated Tolerance to Oxidative Stress and Increases Persister Cell Populations in *Acinetobacter baumannii*. Infect Immun. 2014;82(8):3417-3425. doi:10.1128/IAI.01600-14

35. Nyunda RPB, Wiantini NMR, Susanti NMP, Laksmiani NPL. Comparative in-silico analysis of vitexin and orientin as potential antiphotoaging agents against MMP enzymes. Pharm Rep. 2024;3(2):60. doi:10.51511/pr.60

36. Yu Y, Pei F, Li Z. Orientin and vitexin attenuate lipopolysaccharide-induced inflammatory responses in RAW264.7 cells: a molecular docking study, biochemical characterization, and mechanism analysis. Food Sci Hum Wellness. 2022;11(5):1273-1281. doi:10.1016/j.fshw.2022.04.024

37. Khumbulani M, Alayande KA, Sabiu S. Orientin Enhances Colistin-Mediated Bacterial Lethality through Oxidative Stress Involvement. Evid Based Complement Alternat Med. 2022;2022:1-9. doi:10.1155/2022/3809232

**Table Legends**

**Table 1. Molecular docking binding affinities showing the interactions of the flavonoids** Vitexin and Orientin with *A. baumannii* target regulators. **(1A)** Represents the docking results of Vitexin and Orientin with the 5HM6 transcriptional regulator. **(1B)** Represents the docking results of Vitexin and Orientin with the 7ZL4 chaperone-usher pilus system protein.

**Figure Legends**

**Figure 1. Crystal violet assay showing the antibiofilm activity of P. incarnata extract against CUAB-01. (A)** At concentrations of 0.312 mg/mL and 0.156 mg/mL, the extract inhibited biofilm formation by 52.11% and 25.22%, respectively, while the corresponding bacterial growth percentages were measured at 600 nm. The X-axis represents the extract concentrations (mg/mL), and the Y-axis indicates the percentage of biofilm inhibition and growth. Data are expressed as mean ± SD (n = 3). **(B)** Air–liquid interface biofilm inhibition observed at all tested concentrations of *P. incarnata* extract.

**Figure 2. Inhibitory activity of *P. incarnata* extract on alginate production in CUAB-01.** The extract effectively reduced alginate synthesis, an essential biofilm matrix component, showing maximum suppression at 0.312 mg/mL (40.28%), followed by 0.156 mg/mL (27.96%). Data are presented as mean ± SD (n = 3).

**Figure 3. Growth curve of CUAB-01 treated with *P. incarnata* extract (0.312 mg/mL) compared to the untreated control**. Treatment with the extract showed no significant impact on bacterial growth, as both treated and control cultures exhibited comparable growth patterns over time. Data are presented as mean ± SD (n = 3).

**Figure 4. Inhibition of surface migration and twitching motility in CUAB-01 by *P. incarnata* extract. A)** Swarming motility assay showing a marked reduction in surface migration of CUAB-01 treated with *P. incarnata* extract (0.312 mg/mL) compared to the vigorous swarming displayed by the untreated control. **B)** Twitching motility assay demonstrating a substantial decrease in sub-surface movement in CUAB-01 following treatment with *P. incarnata* extract (0.312 mg/mL) relative to the control.

Results are representative of three biological replicates (n = 3), with consistent inhibition observed across all replicates.

**Figure 5. Effect of *P. incarnata* extract on $H_2O_2$ sensitivity in CUAB-01.** Disc diffusion assay showed a clearance zone of 16 mm in the control plate, which increased to 32 mm following treatment with 0.312 mg/mL extract. Data are representative of three independent biological replicates (n = 3), with consistent trends observed across all replicates.

**Figure 6. Microscopic visualization of biofilm formation in treated and untreated samples.** **(A)** The untreated control of CUAB-01 displayed compact and well-organized biofilm structures after 48 h of incubation. **(B)** Exposure to *P. incarnata* extract at 0.312 mg/mL markedly suppressed biofilm matrix formation.

## Supplementary Tables

### Table Legends

**Table S1. Bond interactions and corresponding lengths from molecular docking studies. (A)** Vitexin interactions with *A. baumannii* regulators 5HM6 and 7ZL4, including the key amino acid residues involved. **(B)** Orientin interactions with *A. baumannii* regulators 5HM6 and 7ZL4, highlighting the participating amino acid residues.

## Supplementary Figures

### Figure Legends

**Figure S1. Docking analysis of Vitexin with *A. baumannii* regulators 5HM6 (A) and 7ZL4 (B).** The figure illustrates (a) docked 3D conformations, (b) BIOVIA-generated 3D interaction profiles, and (c) corresponding 2D interaction visualizations.

**Figure S2. Docking analysis of Orientin with *A. baumannii* regulators 5HM6 (A) and 7ZL4 (B).** The figure presents (a) docked 3D conformations, (b) BIOVIA-generated 3D interaction profiles, and (c) corresponding 2D interaction visualizations.

**Table 1. Molecular docking binding affinities showing the interactions of the flavonoids** Vitexin and Orientin with *A. baumannii* target regulators. **(1A)** Represents the docking results of Vitexin and Orientin with the 5HM6 transcriptional regulator. **(1B)** Represents the docking results of Vitexin and Orientin with the 7ZL4 chaperone-usher pilus system protein.

**(1A)** Represents the docking results of Vitexin and Orientin with the 5HM6 transcriptional regulator.

| **Flavonoid compounds of *P. incarnata*** | **Ligand ID** | **Binding Affinity (kcal/mol)** | **rmsd/ub** | **rmsd/lb** |
|---|---|---|---|---|
| **Vitexin** | **5HM6_A_5280441_uff_E=621.73** | **-6.2** | **0** | **0** |
| Vitexin | 5HM6_A_5280441_uff_E=621.73 | -6.2 | 6.677 | 2.945 |
| Vitexin | 5HM6_A_5280441_uff_E=621.73 | -6 | 6.744 | 2.762 |
| Vitexin | 5HM6_A_5280441_uff_E=621.73 | -6 | 3.957 | 2.463 |
| Vitexin | 5HM6_A_5280441_uff_E=621.73 | -6 | 2.436 | 1.716 |
| Vitexin | 5HM6_A_5280441_uff_E=621.73 | -5.9 | 6.673 | 2.577 |
| Vitexin | 5HM6_A_5280441_uff_E=621.73 | -5.9 | 2.747 | 1.489 |
| Vitexin | 5HM6_A_5280441_uff_E=621.73 | -5.9 | 4.43 | 2.418 |
| Vitexin | 5HM6_A_5280441_uff_E=621.73 | -5.9 | 29.197 | 27.044 |
| **Orientin** | **5HM6_A_5281675_uff_E=472.15** | **-6.6** | **0** | **0** |
| Orientin | 5HM6_A_5281675_uff_E=472.15 | -6.5 | 6.957 | 2.247 |
| Orientin | 5HM6_A_5281675_uff_E=472.15 | -6.3 | 7.58 | 2.495 |
| Orientin | 5HM6_A_5281675_uff_E=472.15 | -6.2 | 5.27 | 3.143 |
| Orientin | 5HM6_A_5281675_uff_E=472.15 | -6.1 | 5.897 | 3.218 |
| Orientin | 5HM6_A_5281675_uff_E=472.15 | -6.1 | 28.991 | 26.332 |

| | | | | |
|---|---|---|---|---|
| Orientin | 5HM6_A_5281675_uff_E=472.15 | -6 | 25.651 | 21.443 |
| Orientin | 5HM6_A_5281675_uff_E=472.15 | -6 | 26.895 | 22.918 |
| Orientin | 5HM6_A_5281675_uff_E=472.15 | -6 | 29.568 | 26.577 |

**(1B)** Represents the docking results of Vitexin and Orientin with the 7ZL4 chaperone-usher pilus system protein.

| **Flavonoid compounds of *P. incarnata*** | **Ligand ID** | **Binding Affinity (kcal/mol)** | **rmsd/ub** | **rmsd/lb** |
|---|---|---|---|---|
| **Vitexin** | **7ZL4_B_985_uff_E=3747.78** | **-6.5** | **0** | **0** |
| Vitexin | 7ZL4_B_985_uff_E=3747.78 | -6.5 | 6.348 | 3.987 |
| Vitexin | 7ZL4_B_985_uff_E=3747.78 | -6.2 | 7.993 | 3.306 |
| Vitexin | 7ZL4_B_985_uff_E=3747.78 | -6.1 | 4.533 | 2.599 |
| Vitexin | 7ZL4_B_985_uff_E=3747.78 | -6 | 7.08 | 4.144 |
| Vitexin | 7ZL4_B_985_uff_E=3747.78 | -5.6 | 3.38 | 2.45 |
| Vitexin | 7ZL4_B_985_uff_E=3747.78 | -5.3 | 7.841 | 5.229 |
| Vitexin | 7ZL4_B_985_uff_E=3747.78 | -5.2 | 17.992 | 13.568 |
| Vitexin | 7ZL4_B_985_uff_E=3747.78 | -5.1 | 10.442 | 5.36 |
| **Orientin** | **7ZL4_B_5281675_uff_E=491.67** | **-8.7** | **0** | **0** |
| Orientin | 7ZL4_B_5281675_uff_E=491.67 | -8.5 | 6.327 | 2.201 |
| Orientin | 7ZL4_B_5281675_uff_E=491.67 | -8.2 | 7.034 | 1.531 |

| | | | | |
|---|---|---|---|---|
| Orientin | 7ZL4_B_5281675_uff_E=491.67 | -8.1 | 14.062 | 9.471 |
| Orientin | 7ZL4_B_5281675_uff_E=491.67 | -8 | 14.658 | 10.586 |
| Orientin | 7ZL4_B_5281675_uff_E=491.67 | -7.7 | 7.738 | 2.168 |
| Orientin | 7ZL4_B_5281675_uff_E=491.67 | -7.5 | 16.142 | 12.026 |
| Orientin | 7ZL4_B_5281675_uff_E=491.67 | -7.4 | 5.769 | 1.785 |
| Orientin | 7ZL4_B_5281675_uff_E=491.67 | -7.4 | 12.451 | 8.437 |

**Figures**

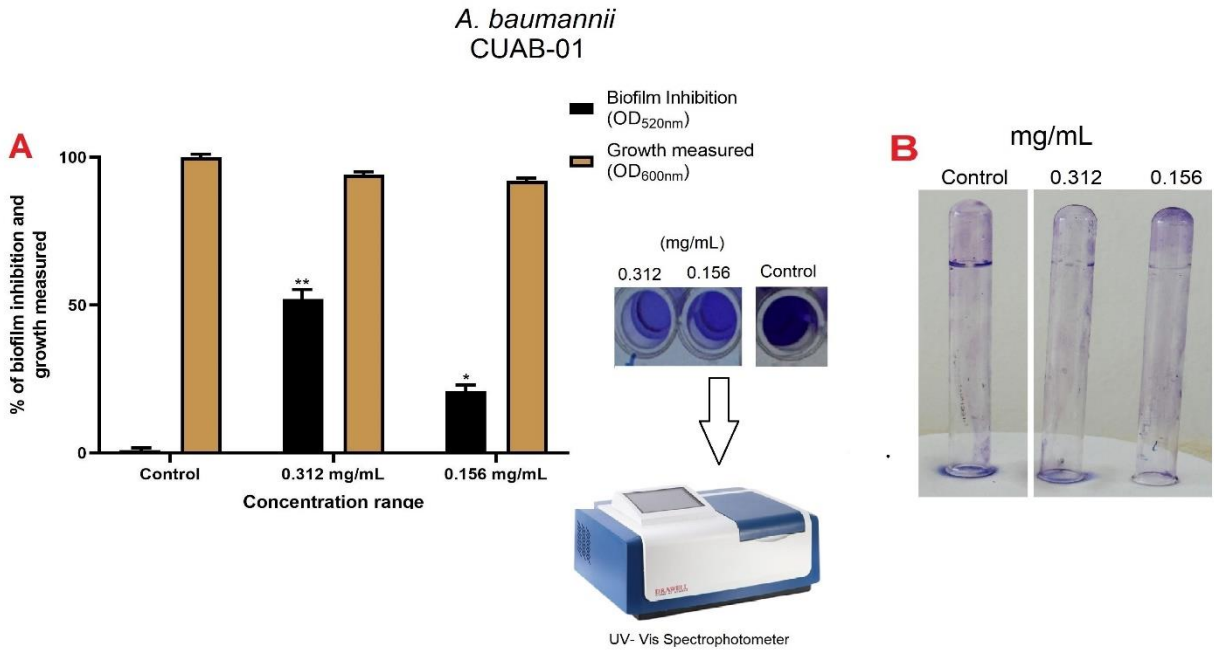


**Figure 1. Crystal violet assay showing the antibiofilm activity of *P. incarnata* extract against CUAB-01. (A)** At concentrations of 0.312 mg/mL and 0.156 mg/mL, the extract inhibited biofilm formation by 52.11% and 25.22%, respectively, while the corresponding bacterial growth percentages were measured at 600 nm. The X-axis represents the extract concentrations (mg/mL), and the Y-axis indicates the percentage of biofilm inhibition and growth. Data are expressed as mean ± SD (n = 3). **(B)** Air–liquid interface biofilm inhibition observed at all tested concentrations of *P. incarnata* extract.

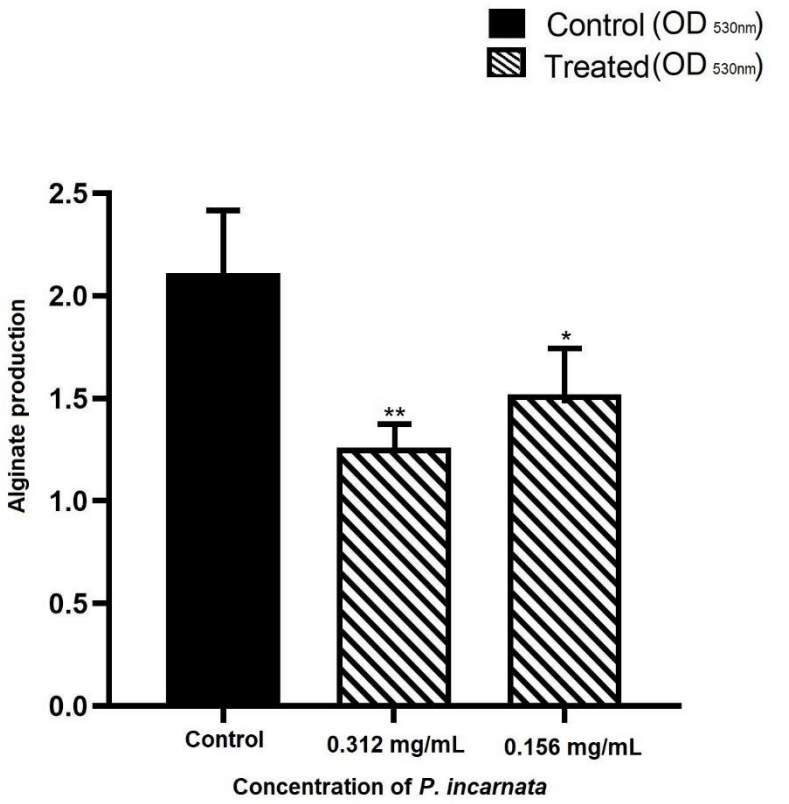


**Figure 2. Inhibitory activity of *P. incarnata* extract on alginate production in CUAB-01.** The extract effectively reduced alginate synthesis, an essential biofilm matrix component, showing maximum suppression at 0.312 mg/mL (40.28%), followed by 0.156 mg/mL (27.96%). Data are presented as mean ± SD (n = 3).

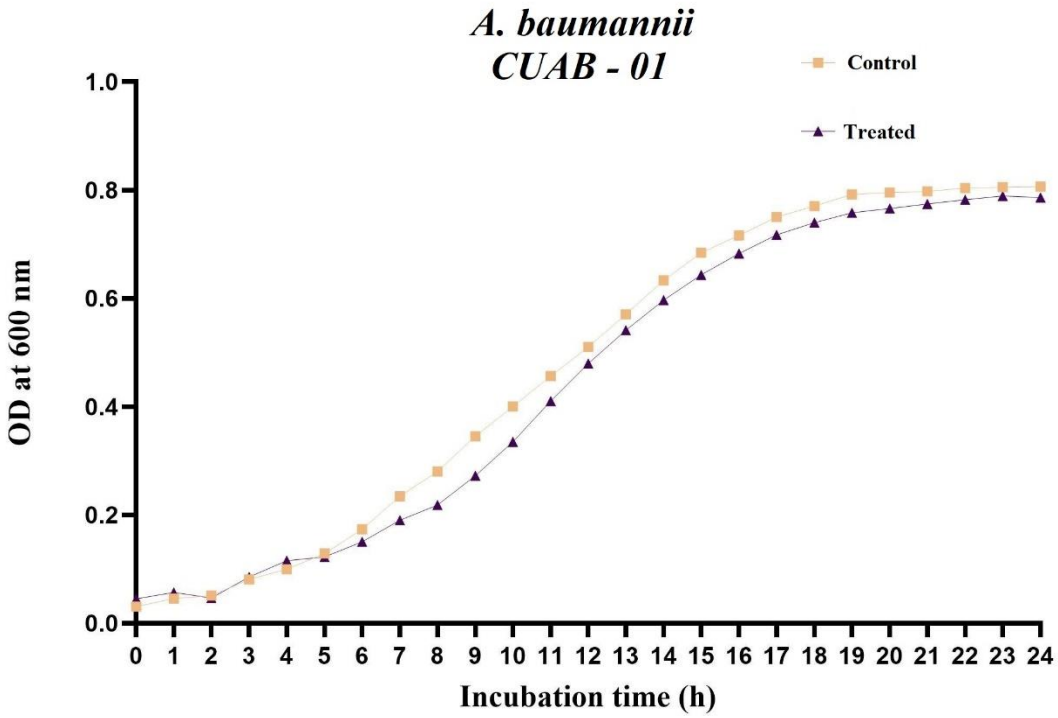


**Figure 3. Growth curve of CUAB-01 treated with *P. incarnata* extract (0.312 mg/mL) compared to the untreated control.** Treatment with the extract showed no significant impact on bacterial growth, as both treated and control cultures exhibited comparable growth patterns over time. Data are presented as mean ± SD (n = 3).

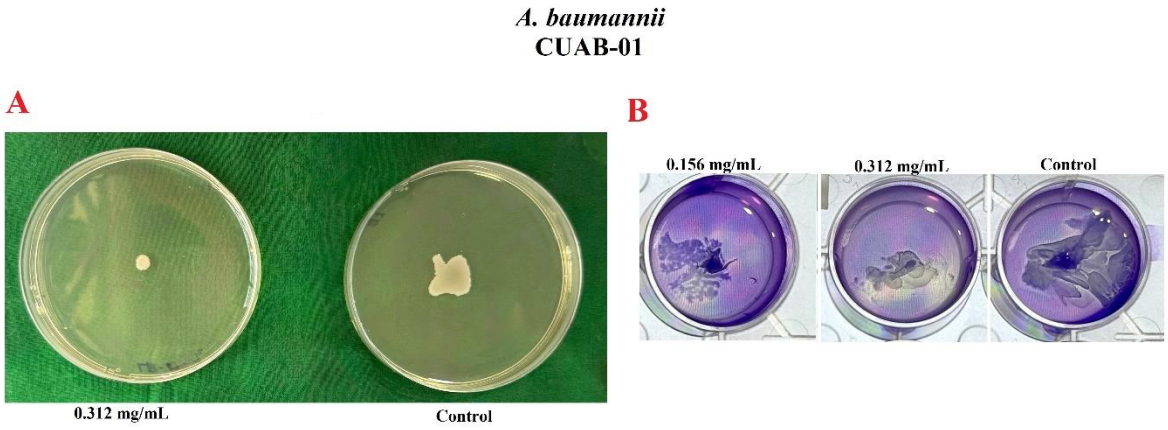


**Figure 4. Inhibition of surface migration and twitching motility in CUAB-01 by *P. incarnata* extract. A)** Swarming motility assay showing a marked reduction in surface migration of CUAB-01 treated with *P. incarnata* extract (0.312 mg/mL) compared to the vigorous swarming displayed by the untreated control. **B)** Twitching motility assay demonstrating a substantial decrease in sub-surface movement in CUAB-01 following treatment with *P. incarnata* extract (0.312 mg/mL and 0.156 mg/mL) relative to the control.

Results are representative of three biological replicates (n = 3), with consistent inhibition observed across all replicates.

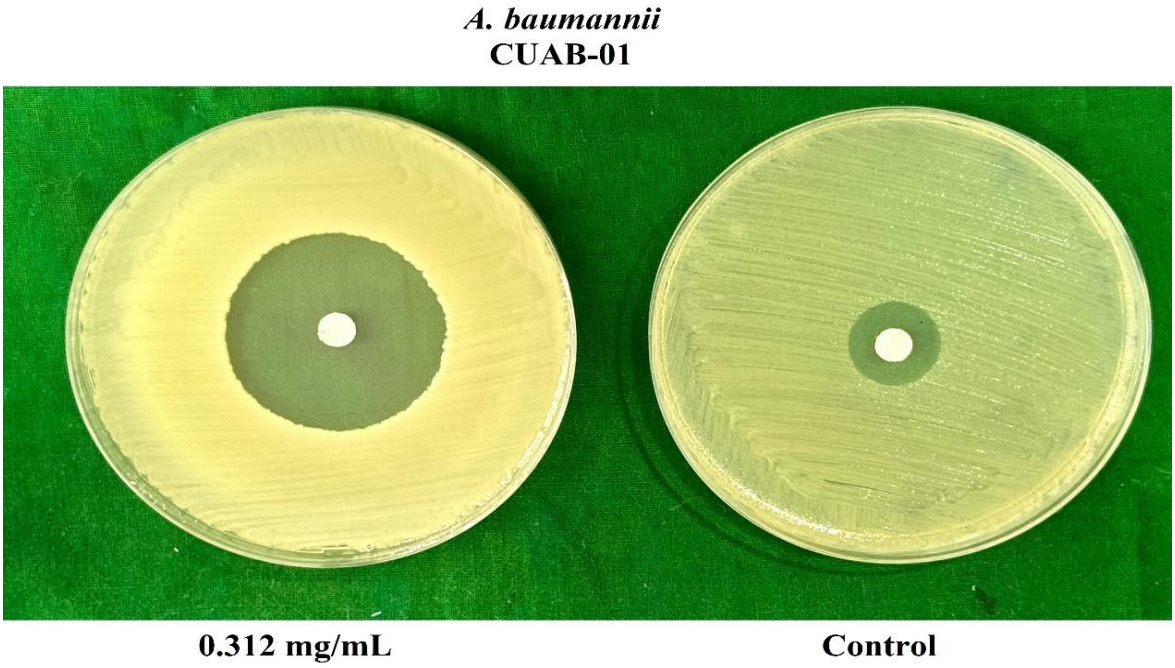


**Figure 5. Effect of *P. incarnata* extract on $H_2O_2$ sensitivity in CUAB-01.** Disc diffusion assay showed a clearance zone of 16 mm in the control plate, which increased to 32 mm following treatment with 0.312 mg/mL extract. Data are representative of three independent biological replicates (n = 3), with consistent trends observed across all replicates.

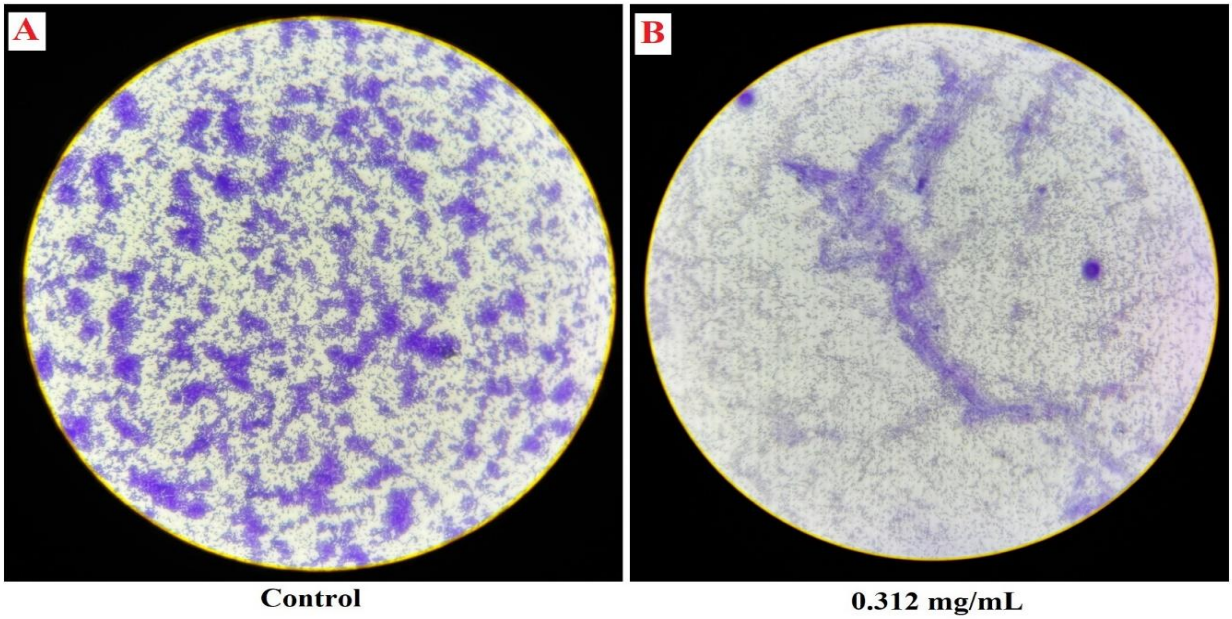


**Figure 6. Microscopic visualization of biofilm formation in treated and untreated samples.** **(A)** The untreated control of CUAB-01 displayed compact and well-organized biofilm structures after 48 h of incubation. **(B)** Exposure to *P. incarnata* extract at 0.312 mg/mL markedly suppressed biofilm matrix formation.